Rigid-flexible contact analysis of an inflated membrane balloon with various contact conditions

M. X. Liu[1] and X. D. Li[1,*]

[1] Department of Engineering Mechanics, Tsinghua University, 100084, China,

Emails: lmxyj0034@163.com and lixide@tsinghua.edu.cn.

[*] Correspondence: lixide@tsinghua.edu.cn.

† Presented at **ICEM2018, Brussels, July 4th**

Abstract

Considering the Mooney–Rivlin hyperelastic model, a semi-analytical approach is introduced to analyze the rigid–flexible contact behaviors of an inflated membrane balloon between two plates with various interface conditions. This approach is based on the differential formulation and the coupling property of equilibrium equations are well-solved. In order to verify the reliability of the proposed theoretical model, an experimental test is designed, by which some important contact characteristics and patterns (no-slip condition) are obtained. Two special phenomena are observed for the meridian stretch ratio with different friction coefficients. One is that the intersection points of all curves fall in a small interval and the intersection of any two curves represents the same changing rate of the horizontal ordinate, resulting in the maximum difference. The other is the dividing point, where the stretch ratio decreases on the left of it and increases on the right due to the introduction of friction. These results provide solid guidance and support for our understanding of the rigid-flexible contact behaviors of an inflated membrane balloon.

Keywords: Mooney–Rivlin hyperelastic membrane; the differential formulation; stick-slip condition

1. Introduction

As the typical membrane structure, inflated balloon has considerable importance in a number of scientific studies and technological applications. On the macro scale, it can be used in terrestrial and space structures due to the advantages of light-weight, quick and self-deployment, and compact storage properties [1] (Jenkins, 2001). On the micro scale, it can be used as animal or plant cell [2] (Moretti et al., 2004).

The investigations on the contact behaviors of an inflated membrane can be summarized as two processes: geometry nonlinearity analysis and boundary condition nonlinearity analysis. The geometry nonlinearity is carefully considered by solving the membrane inflation problem [3] (Feng and Yang, 1970). Moreover, a lot of works have been done to deal with the nonlinearity problem of the boundary condition [4] (Feng and Yang, 1973, Johnson, Kendall and Roberts, 1971). Broadly, solution schemes proposed to this problem are divided into two categories: finite element analysis and semi-analytical approach. Based on the finite element method, the membrane large

1

deformation problems, nonlinear static behaviors, inflation and contact characteristics are analyzed by Leonard and Verma (1976) [5] and Charrier and Shrivastava (1987) [6]. On the basis of different contact models (Yang and Feng, 1973; Patil and DasGupta, 2015) [7], the contact problems are simplified to a set of ordinary differential equations, which can be solved by numerical methods.

In the existing literature, diverse methods are proposed based on the variational formulation. The coupled normal adhesive force and tangential friction force will increase the difficulty of the solving process. To deal with this problem, a semi-analytical method rooted in the differential formulation is introduced to extend the modal of Feng and Yang (1973) [8] and more complex contact boundary conditions are studied.

2. Geometry and constitutive models

A spherical balloon with uninflated radius r_0 and uniform thickness h (state I the black line) is inflated to radius r_s by pressure P_0 (state II the red line). Then two parallel rigid plates are pressed by F into contact with the balloon (state III the green line). Half of the spherical balloon and one rigid plate are shown in Fig. 1. The inflated spherical balloon before contact is described by the spherical coordinates (r_s, β, α). The cylindrical coordinates (ρ, β, η) are used for the spherical balloon after contact.
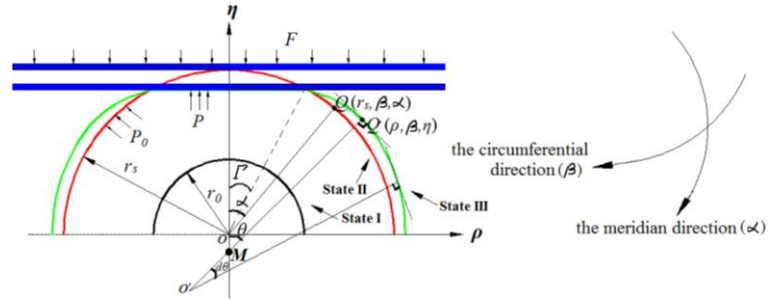

Fig.1 the contact model of an inflated membrane and rigid plates

The governing differential equations are built for the non-contact region and the contact one, separately.

In the non-contact region: according to the geometric relation, the principal stretch ratios for the membrane can be written as $\lambda_\alpha, \lambda_\beta$. Here, the subscripts α and β denote the meridian and circumferential directions.

$$\lambda_\alpha = \frac{dS}{ds} = \frac{\sqrt{\rho'^2 + \eta'^2}}{r_0}, \qquad \lambda_\beta = \frac{\rho}{r_0 \sin \alpha}. \tag{1}$$

The prime in the foregoing and subsequent equations denotes the derivatives with respect to the angle α.

The structure is considered as the non-moment thin shell, which has no bending moment and torsion on the cross section, and the equilibrium differential equations can be expressed due to the constitutive relation and the axial symmetry.

$$\frac{dT_\alpha}{d\rho} + \frac{T_\alpha - T_\beta}{\rho} = \frac{P_t}{\cos \theta},$$
$$\kappa_\alpha T_\alpha + \kappa_\beta T_\beta = P_n, \tag{2}$$

where $P_n = q_n$ and $P_t = q_\alpha$ are the external loads acting on the deformed surface in the normal and meridian tangential directions.

Based on the Mooney-Rivlin hyperplastic constitutive model, the equilibrium equations can also be obtained due to the new defined variables: $\delta = \lambda_\beta \sin\alpha, \ \omega = \delta', \ \bar{h} = \dfrac{h}{r_0}, \ p = \dfrac{P}{C_1}$ (Feng and Yang (1973)):

$$\lambda_\alpha' = \frac{\lambda_\alpha^4 \delta^3}{(\lambda_\alpha^4 \delta^2 + \sin^2\alpha)\sin\alpha} \left\langle \begin{array}{l} (\delta'\sin\alpha - \delta\cos\beta)(\dfrac{\lambda_\alpha}{\delta^2} - \dfrac{3\sin^2\beta}{\lambda_\alpha^3\delta^4}) - \\[2mm] \dfrac{1}{1 + \dfrac{\varsigma\delta^2}{\sin^2\alpha}} \left\{ \begin{array}{l} \dfrac{2\varsigma\delta}{\sin\alpha}(\dfrac{\lambda_\alpha}{\delta} - \dfrac{\sin^3\alpha}{\lambda_\alpha^3\delta^3})(\delta' - \dfrac{\delta\cos\alpha}{\sin\alpha}) - \\[2mm] \dfrac{\delta'}{\delta}\left[\begin{array}{l} \varsigma\left(\dfrac{\sin\alpha}{\lambda_\alpha^3\delta} - \dfrac{\sin^3\alpha}{\lambda_\alpha\delta^3}\right) + \\[2mm] (\dfrac{\delta}{\lambda_\alpha\sin\alpha} - \dfrac{\lambda_\alpha\sin\alpha}{\delta}) \end{array}\right] \end{array}\right\} \end{array}\right\rangle, \quad (3)$$

$$\delta' = \omega,$$

$$\omega' = \frac{\omega\lambda_\alpha'}{\lambda_\alpha} + \frac{\lambda_\alpha^4\delta^3\sqrt{\lambda_\alpha^2 - \omega^2}}{(\lambda_\alpha^4\delta^2 - \sin^2\alpha)(\sin\alpha + \dfrac{\varsigma\delta^2}{\sin\alpha})} \left\{ \begin{array}{l} \dfrac{1}{\lambda_\alpha\delta}\sqrt{\lambda_\alpha^2 - \omega^2}(\dfrac{\delta}{\lambda_\alpha\sin\alpha} - \dfrac{\sin^3\alpha}{\lambda_\alpha^3\delta^3}) \times \\[2mm] (1 + \varsigma\lambda_\alpha^2) - \dfrac{p}{2\bar{h}} \end{array}\right\}.$$

In the contact region: for the complex stick-slip contact condition, it becomes the frictionless contact condition when the friction coefficient becomes zero. If the friction coefficient goes to infinity, it is converted into the no-slip contact condition. Then, this contact condition is considered in this paper. Because the friction coefficient is limited, material will stick when the interfacial friction is greater than the membrane tension, while the others will slip.

$$\lambda_\alpha' = \frac{1}{\left(\dfrac{1}{\lambda_\beta} + \dfrac{3}{\lambda_\alpha^4\lambda_\beta^3}\right)(1 + \varsigma\lambda_\beta^2)} \left\{ \begin{array}{l} \dfrac{\lambda_\alpha - \lambda_\beta\cos\alpha}{\sin\alpha} \left[\begin{array}{l} \left(\dfrac{\lambda_\alpha}{\lambda_\beta^2} - \dfrac{3}{\lambda_\alpha^3\lambda_\beta^4}\right)(1 + \varsigma\lambda_\beta^2) - \\[2mm] 2\varsigma\lambda_\beta\left(\dfrac{\lambda_\alpha}{\lambda_\beta} - \dfrac{1}{\lambda_\alpha^3\lambda_\beta^3}\right) \end{array}\right] + \\[4mm] \dfrac{\lambda_\alpha}{\lambda_\beta\sin\alpha}\left[\left(\dfrac{\lambda_\beta}{\lambda_\alpha} - \dfrac{\lambda_\alpha}{\lambda_\beta}\right) + \varsigma\left(\dfrac{1}{\lambda_\alpha^3\lambda_2} - \dfrac{1}{\lambda_1\lambda_2^3}\right) - \dfrac{r_0\lambda_1\mu_f P}{2C_1 h}\right] \end{array}\right\}, \quad (4)$$

$$\lambda_\beta' = \frac{\lambda_\alpha - \lambda_\beta\cos\alpha}{\sin\alpha}.$$

The equilibrium equation along the meridian tangential direction of the spherical balloon in the contact region can be rewritten as $\dfrac{dT_\alpha}{d\rho} + \dfrac{T_\alpha - T_\beta}{\rho} = \tau$. Hence, the equilibrium condition for the critical sliding state can be obtained.

3. Results and discussion
3.1 Experiment verification

In order to verify the theoretical results, a testing scheme is proposed to measure the patterns and some important contact characteristics of the inflated balloon.

Before the experiment, the speckle pattern on the balloon is reproduced artificially. To increase the contrast of the speckle, matte white paint and black paint are sprayed on the balloon surface evenly. In the experiment, the balloon with sprayed speckles is placed on the workbench and its position is adjusted so that it is on the compression axis. After that, the balloon is inflated by the pump. The displacement load is applied to the balloon, which can be controlled precisely by the electronic universal testing machine. This load is noted down by a ruler on the machine and the internal pressure of the balloon is

monitored by the barometer (Fig. 2). The deformations of the balloon are tested using the digital image correlation (DIC) technology, which is a reliable mean to measure the displacement fields.

Tab. 1 Material and geometrical parameters

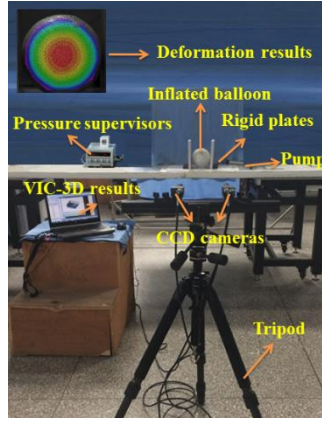| Parameters	Magnitude
Initial radius (r_0)	0.05 (m)
Thickness of the beam (h)	0.3(mm)
Young's modulus of membrane(E)	6 (MPa)
Poisson's ratio (ν)	0.47
Stretch ratio before contact (λ_s)	3

Fig. 2 setup of the contact experiment

The maximum displacement of the balloon ($\alpha = \pi/2$) is compared in Tab. 2 and deformation contours of the balloon are obviously observed and tested in the in Fig. 3.
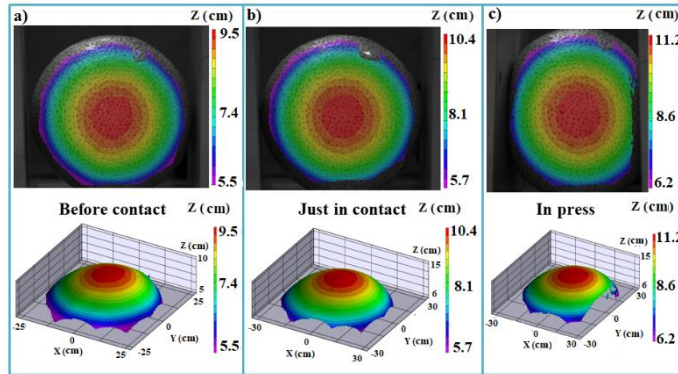

Fig. 3 three stages of contact (a) before contact b) just in contact c) in press)

Tab.2. the experimental and theoretical results of the maximum displacement under different displacement load

	Displacement load (cm)	0.63	2.13	4.25
maximum displacement ($1/r_0$)	theoretical results	2.05	2.18	2.34
	experimental results	2.08	2.25	2.50

When the inflated balloon is just in contact to plates, the maximum displacement appears in the middle ($\alpha = \pi/2$). The tested deformation (10.4cm) agrees with the theoretical result (10.0cm) with an error around 0.33%. When the displacement load is

4.25cm, the error reaches to the maximum, which is 6.8%.

3.2 Theoretical prediction

As a general case, the results from the stick-slip contact condition are mainly discussed in this section.

For different friction coefficients, the changing trend of the meridian stretch ratio λ_α with the angle α is shown in Fig.4, where the contact angle is $60°$.

Two special phenomena can be seen in Fig.4. One is that the intersection points of all curves fall in a small interval, and the other is the dividing point ($\alpha = \text{angle} = 1.05$). The intersection point of any two curves appears in the contact region, which represents that material have the same meridian stretch ratio under the conditions with corresponding friction coefficients at that point. Moreover, different from the condition of $\mu_f = 0$, a dividing point, which is the boundary of contact and non-contact regions, appears when friction is introduced.
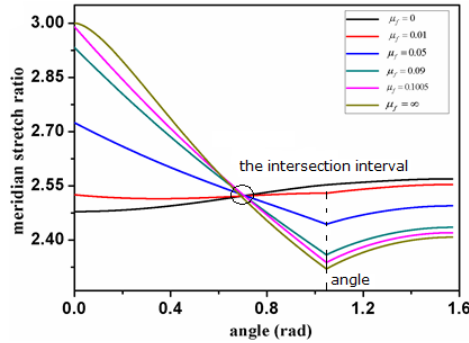

Fig.4 the changing trend of meridian stretch ratio λ_α with angle α in different
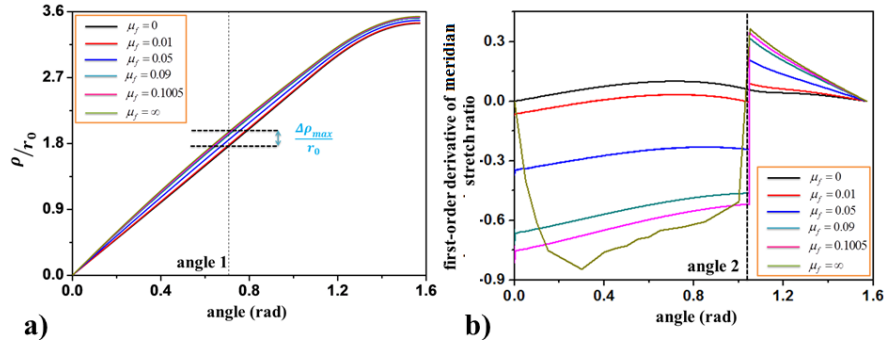
friction coefficient conditions.

Fig.5 a) horizontal ordinate ρ/r_0 and angle relationship with different friction

coefficients b) the horizontal ordinate difference $\Delta\rho/r_0$ between introduced friction

conditions (different coefficients) and frictionless one

To better explain the intersection interval in Fig.4, the relationship between the horizontal ordinate and angle is counted in Fig.5 a) and the horizontal ordinate difference between the introduced friction conditions and the frictionless one is described in Fig.5 b). In the contact region, the relationship $\lambda_\alpha = \rho'/r_0$ is satisfied. Then the intersection of

any two curves represents the same changing rate of the horizontal ordinate ρ/r_0, resulting in the maximum difference at that point.

Moreover, a step point appears at $\alpha = angle = 1.05$ in Fig.4, which is corresponding to the dividing point between the contact and non-contact regions Fig.5 b). This means the changing trend of the meridian stretch ratio is different in the contact and non-contact regions, though this stretch ratio changes continuously in these two regions.

Conclusions

In this paper, a semi-analytical approach based on the force equivalent method is introduced to the Mooney–Rivlin hyperelastic membrane modal to characterize the rigid-flexible contact behaviors of an inflated membrane balloon. In the contact region, the typical stick-slip condition is considered. The inflatable and contact process can be tracked using the proposed model. The patterns and characteristics before contact, just in contact and in press can be verified by the experimental tests.

Considering the particularity of the stick-slip contact condition, the friction plays an important role. A small intersection interval appears in the meridian stretch ratio for different friction coefficients in the contact region and the horizontal ordinate changing ratio of any two conditions with different friction coefficients keeps the same, resulting in the maximum difference of this ordinate. Unlike the increasing meridian stretch ratio with the increment of the angle when friction coefficient is zero, a dividing point appears between the non-contact and contact regions when the friction is introduced. It declines in the contact region and increases in the non-contact region because of the interface friction, which prevents material of the balloon from sliding to the pole.

Reference

1. Jenkins, C. Gossamer spacecraft (membrane and inflatable structures technology for space applications). Progress in Astronautics and Aeronautics **2001**.

2. Moretti, M.; Prina-Mello. Endothelial cell alignment on cyclically-stretched silicone surfaces. Journal of Materials Science: Materials in Medicine **2004**, 15, 1159–1164, DOI: 10.1023.

3. Yang, W. H.; Feng, W. W. On axisymmetrical deformations of nonlinear membranes. Journal of Applied Mechanics **1970**, 37, 1002–1011, doi:10.1115/1.3408651.

4. Johnson, K. L.; Kendall, K.; Roberts, A. D. Surface energy and the contact of elastic solids. Proceedings of the Royal Society of London A **1971**, 324, 301-313, DOI: 10.1098/rspa.1971.0141.

5. Leonard, J. W.; Verma, V. K. Double-curved element for Mooney-Rivlin membranes. Journal of the Engineering Mechanics Division **1976**, 102, 625-641.

6. Charrier, J. M.; Shrivatava, S. Free and constrained inflation of elastic membranes in relation to thermoforming axisymmetric problem. The Journal of Strain Analysis for Engineering Design **1989**, 24, 55–74.

7.Patil, A.; DasGupta, A.; Eriksson, A. Contact mechanics of a circular membrane inflated against a deformable substrate. International Journal of Solids & Structures **2015**, 67, 250-262, DOI: 10.1016.

8. Feng, W. W.; Yang, W. H. On the contact problem of an inflated spherical nonlinear membrane. Journal of Applied Mechanics **1973**, 40, 209-214, DOI:10.1115/1.3422928.